Tumour Detection By Volumetric Image Analysis

Ashley J. Robinson

University of Southampton

ajr2g10@ecs.soton.ac.uk

Abstract—This research review covers techniques available for detecting tumours in the human body considering practical implications of concatenated methods. An architecture is proposed in order to give direction to research and to allow consideration of processing interactions. Targeted at medical review applications the system follows standard image processing conventions and contains a sub-module that provides confidence information for a domain expert. Volumetric image processing techniques for pre-processing and feature extraction are reviewed. Machine learning techniques for feature selection and classification are also considered.

The recommendation for population begins with anisotropic diffusion, for edge preservation smoothing, followed by edge, curvature and shape extraction. Leading to principal component analysis for dimensionality reduction then finally a support vector machine for classification. The AdaBoost algorithm is considered for improving classifier performance and further pruning the input space. Human supervised deployment is considered, after further testing, whether stand-alone or as an extension to existing medical review software.

I. Introduction

THIS research review covers the use of volumetric image analysis in medicine to accurately detect the presence of tumours in the human body. The problem is to be approached by considering the general cases therefore concentration is not set on a specific area of the body. Rather than trying to classify lung or brain tumours individually the goal is to consider what features tumours have in common and given an entire image of a human body is it possible to classify the presence of a tumour in any given section? The motivation behind this is to make the most of medical scanning. Dosages of radiation, cost and capture time are all reasons to reduce the number of required patient scans. Throughly inspecting any data gathered is a constructive method of scan reduction. A practical end objective is used to provide direction to research and maximise the resultant impact which is to provide a recommendation for a tool to be implemented that can assist with medical practitioner diagnosis.

The architecture in Fig. 1 is the framework of the system to be recommended and is inspired by similar topologies discussed in the literature [1]–[5]. A chain of stages leads from raw data gathered from the patient to a classification algorithm resulting in diagnosis. A confidence sub-block enables an expert to view the performance of the entire system without knowing the intricacies of operation which means processing is required for domain translation. In machine learning for medical applications a classification threshold has to be selected carefully as false negatives are more serious the false positive.

Raw data is captured from the patient and passed to the system for pre-processing then feature extraction. Input patterns are produced dependent on a pre-determined list of known useful tumour features. Dimensionality reduction is then used to frame the data as such to make the most of the classification algorithm.
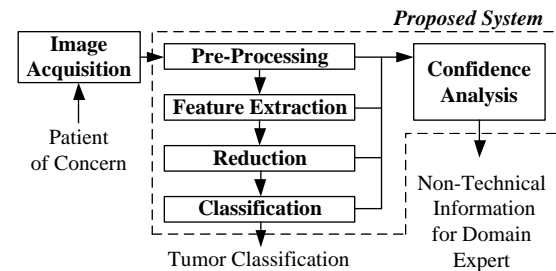

Fig. 1. Proposed system architecture.

II. Image Acquisition

A standard medical X-ray is tuned to produce an image of human bone. The rays are attenuated by different materials in the body, more so by dense regions, and the image is gained from this attenuation effect [6]. This uses a single source and substrate pair to capture the image. Taking multiple images from many different angles gathers more information and a 3D image can be made by stitching these together. Fig. 2 describes the physical process of gathering data to be used in Computed Tomography (CT). A ring allows images to be capture from 360° in a single plane then by moving in the orthogonal plane is is possible to compute a full volumetric image.
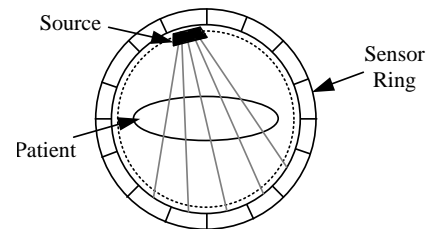

Fig. 2. Acquiring data from Computed Tomography [6].

Any method of non-invasive image capturing in 2D can therefore be expanded to work in 3D by using the CT principle. Different methods have trade-offs such as radiation dosages and resolution. Ultrasound is a method of image acquisition which does not use electromagnetic radiation and requires little computational processing. This means internal organs can be viewed in real-time which is beneficial because it allows practitioners to view internal physical movement. It can be

used for CT but higher resolution methods are usually favoured such as X-ray and Magnetic Resonance Imaging (MRI).

There are also other non-intrusive methods that do not use electromagnetic or ultrasonic waves. Hand palpitation is a common technique used by medical practitioners to gain an impression of abnormalities near the surface of the human body. Electromechanical apparatus employing the same technique can be used to transfer the geometry of a growth to a volumetric image [7], [8]. Only part of the area under inspection is visible so the technique has obvious drawbacks.

Only high resolution grayscale sources will be considered in this review. This data is typically stored as a series of 2D images which are scan slices. An image viewer will build 3D images as and when required. The common medical standard for these images is DICOM which holds the slices, relative position and also the patient's details [9]. Viewing an image naturally proves problematic because it is 3D data shown in an isometric fashion on a 2D screen. Software provides interactive rendering as shown in Fig. 3 which allows the user to move three planes to gain an impression of a region.
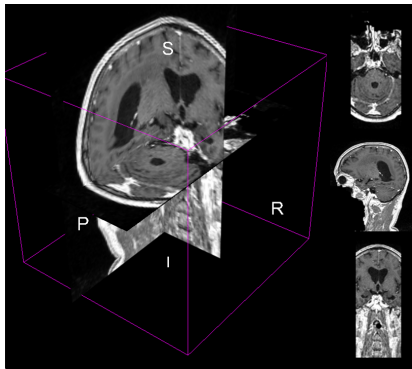

Fig. 3. An MRI scan of a healthy brain taken from and rendered by image review software [10], [11].

III. TUMOUR FEATURES

There are hundreds of types of tumours that can occur in the human body but they are all caused by abnormalities in cell growth [12]. Tumours are dense areas of cells and can be either benign or malignant. Malignant tumours are considered cancers because they invade nearby normal tissue and spread therefore making them an area of concern. These are broken down in to three categories. *Carcinomas*, cells lining the body and internal organs, account for 90% of human caners. *Leukemias* and *Lymphomas*, occurring in the blood and lymph systems, account for 8% in humans. *Sarcomas* are solid regions of connective tissue which are rare.

All types of tumours are areas for concern. Fig. 4 shows an initial accelerated growth rate producing a benign tumour which eventually becomes malignant as it spreads to nearby tissue. Malignant tumours and carcinomas in situ can be easily removed by surgery. Once a tumour begins to metastasize surgery becomes ineffective. Detection should be tuned towards the dense regions, Fig. 4(b), before spreading and when spread locally so surgery remains a viable solution.

(a) Hyperprolifera-tion cell population. (b) Small adenoma (benign). (c) Large adenoma plus carcinoma (malignant).
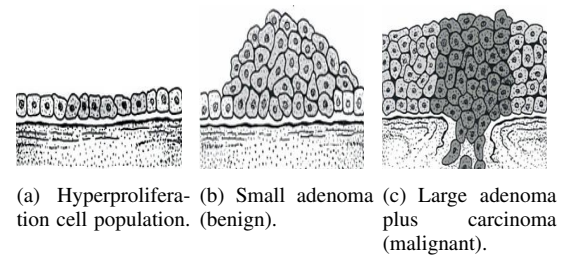
Fig. 4. Development of colon/rectum carcinomas [12].

Whether the tumour lines the host or grows independently the key to identification is to differentiate normal and abnormal cell density. Fig. 5 contains examples of identified tumours in different organs. Tumours shown in the brain and lungs, Fig. 5(a) and 5(c), are far simpler to identify than the liver example image in Fig. 5(c). An image of a liver will contain other organs so these must be considered when trying to extract features.
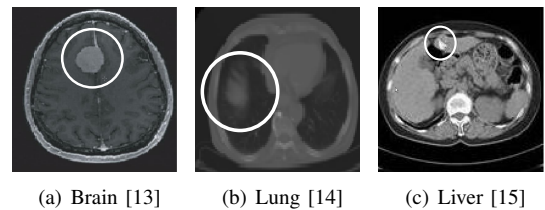

(a) Brain [13]   (b) Lung [14]   (c) Liver [15]

Fig. 5. Example MRI images containing tumours.

IV. PRE-PROCESSING

The analogue of a pixel (picture element) in a 2D image is called a voxel (volumetric element) in a 3D image. This is exactly the same idea but with a extra dimension to form a cube [16]. They can be considered cubes but also points which may make visualisation and processing easier to understand. Fig. 6 describes how voxels are packed and the three different neighbourhoods that can be considered when inspecting a single voxel. Considering voxels to have larger neighbourhoods can increase the time complexity of some algorithms.
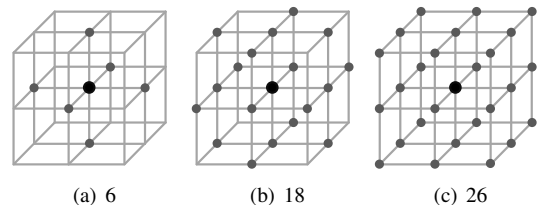

(a) 6   (b) 18   (c) 26

Fig. 6. Voxel Neighbourhoods [16].

The raw data provided needs to be converted from the delivery format of the acquisition technology to a raw 3D matrix ready for generic processing. Watermarking, which may have been inserted for human review, should also be removed at this stage. This is trivial in theory but requires a database of artefacts or manual review to accomplish. There are also

techniques, not considered in this report, which can be applied only to the slices of volumetric images therefore reducing computation overheads [17].

Pre-processing methods are used to enhance the image captured and ensure it is correctly formatted for further processing. This is considered as an image mapping, $\mathbf{I} \mapsto \mathbf{I}'$, using only information from the original image.

A. Histogram Operations

In this context a histogram is a mapping from the image to cumulative voxel intensity. This is possible because voxels only have discrete values of intensity within a fixed range. Some materials can be determined from image intensity therefore a histogram contains information on the quantity of a given material contained in the image. Image enhancement can be performed using point operations with information from the histogram. This is a fast enhancement method as it is direct voxel-to-voxel mapping as shown in Eq. (1). Normalisation stretches the histogram to cover all available values of intensity therefore improving contrast. Equalisation attempts to flatten the histogram by distributing intensity [18].

$$I'(u,v,w) = \alpha(u,v,w)I(u,v,w) \tag{1}$$

B. Spatial Filtering

Spatial filters use the neighbourhood of voxels to create a new value for each voxel in an image. The original image is mapped through a filter kernel as described in Eq. (2). The filter kernel is a fixed dimension sub-image with a weighting on each voxel that is applied to every voxel in the original image. This is spatial convolution. If the filter kernel contains all ones it is known as a *box filter* and performs smoothing on the image to remove noise. A Gaussian filter performs better by placing a higher weighting on the central voxel and less weighting on the edge voxels inside the kernel [16]. The edge voxels of an image do not have a complete set of neighbours therefore performing spatial filtering will reduce the total size of the image in further processing.

$$I'(u,v,w) = \sum_{(i,j,k) \in R_H} I(u+i, v+j, w+k)H(i,j,k) \tag{2}$$

C. Frequency Filtering

The Fourier transform, as used spatially on 2D images, can be extended to 3D images. A Discrete Fourier Transform (DFT) for an N^3 voxel image is held in Eq. (3). The spatial filtering process performs convolution so once an image is in the frequency domain the same effects can be achieved using multiplication. It may prove more efficient to filter an image in the frequency domain rather than the spatial domain if the required filter kernel is large. Band-pass and notch filter operations can also be performed in the frequency domain.

Eq. (4) provides the same result as Eq. (2) where $\mathcal{F}$ is described by Eq. (3).

$$F_{u,v,w} = \frac{1}{N^{\frac{3}{2}}} \sum_{x=-\frac{N}{2}}^{\frac{N}{2}-1} \sum_{y=-\frac{N}{2}}^{\frac{N}{2}-1} \sum_{z=-\frac{N}{2}}^{\frac{N}{2}-1} I_{x,y,z} e^{-j\frac{2\pi}{N}(ux+vy+wz)}$$

$$\tag{3}$$

$$\mathbf{I}' = \mathcal{F}^{-1}(\mathcal{F}(\mathbf{I}) * \mathcal{F}(\mathbf{H})) = \mathcal{F}^{-1}(\mathbf{I} * *\mathbf{H}) \tag{4}$$

D. Anisotropic Diffusion

Anisotropic diffusion is a powerful technique used to enhance images where it is possible to remove noise yet retain edges. The technique has been expanded from common 2D applications to 3D medical usage on MRI data [19]. The diffusion effect has the same outcome as a low pass filter with reasonably adjusted values for Δt and the decay constant. The spatial scaler $\mathbf{k}$ is a function of the image and must preserve edges by setting $k(u_{edge}, v_{egde}, w_{edge}, t) = 0$. Using Eq. (5) an iterative approach is provided in Eq. (6) where the original image is the value of $\mathbf{I}$ at time zero. Iteration monitoring and reasonable scalar values in the function $\mathbf{k}$ are required to produce a good outcome. Edge detection methods to be used for $\mathbf{k}$ are discussed in section V-A.

$$\frac{\partial \mathbf{I}}{\partial t} = \mathbf{k}(\mathbf{I})\nabla^2\mathbf{I}, \ \ \mathbf{k}, \mathbf{I} \in \mathbb{R}^4 \tag{5}$$

$$\mathbf{I}_{t+\Delta t} = \mathbf{I}_t + \Delta t \mathbf{k}(\mathbf{I}_t)\nabla^2\mathbf{I}_t \tag{6}$$

V. Feature Extraction

High level feature extraction of volumetric shapes should be used on the input image. Extracted regions may include organ walls or bones but should also include potential tumours.

A. Edge Detection

Edge detection can be performed using convolution with a kernel template as discussed in section IV-B. These templates are designed to create a new image containing voxel differences and can therefore be thought of as taking the derivative of the image. 2D templates are common and can be expanded for volumetric images [18]. As all dimensions must be considered during differencing the 3D application is extended in the third dimension as shown in Fig 7. Smaller filter masks are also available to reduce computation but with dimimnished results.
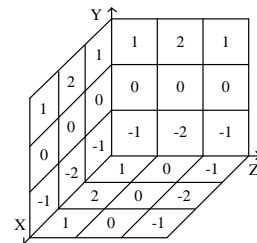

Fig. 7. 3D Sobel filter mask [16].

In edge critical processing better results can be produced with Canny edge detection [20]. A four stage process that uses Gaussian smoothing, the Sobel operator, non-maximal suppression followed by hysteresis thresholding. This reduces noise, minimises position difference in the mapping and eliminates multiple responses to an edge.

B. Curvature Detection

The output of an edge detection method can be measured with respect to curvature. Tumours are expected to differ from the expected flat surfaces of organ walls, measuring curvature will be useful for classification. Curvature can be expressed as the rate of change in the normal along a line, $g(t)$, which is described by Eq. 7. Surface measurements, required in volumetric detection, contain infinitely many curves at a given point [16]. The principle directions, those of most and least curvature, are evaluated then by taking the mean and Gaussian values, $H = (k_1 + K_2)/2$ and $K = k_1 K_2$, so that the category of curvature at a point can be detected. On a plane $H = 0$, $K = 0$, on a peak $H < 0$, $K > 0$ and at a saddle point $K < 0$. An absolute value of curvature can be taken as $E_c = |H| + |K|$.

$$k = \frac{g''(t)}{(1 + g'(t)^2)^{\frac{3}{2}}} \quad (7)$$

C. Hough Transform (HT)

The HT uses a dual space as an accumulator for evidence based location of a shape inside an image [18]. It has been successfully applied to 3D images to locate spherical shapes [21]. Some tumours, Fig. 5(a), grow spherically so the ability to fit a sphere is a useful feature for classification. The distribution of the accumulator space can be used to indicate how many potential spheres fit the image but this is expected to be noisy as it is unlikely tumours will be exact spheres.

D. Active Contours

The active contour model is a method for flexible shape extraction. Expanding upon common 2D implementations active contours can be used to extract features from volumetric images. Eq. (8) contains the standard energy minimisation function [18], [22].

$$E = \int_0^1 E_{int}(\mathbf{v}) + E_{ext}(\mathbf{v}) + E_{con}(\mathbf{v}) \, ds, \; \mathbf{v}(s) \in \mathbb{R}^3 \quad (8)$$

The internal energy is measured using the first and second order differentials of the contours. Eq. (10) contains internal energy with two parametric functions chosen prior to fitting. These control elasticity, α, and stiffness, β, of the contour. The external energy is effected by three variables. Image intensity is controlled by the sign of w_l which attracts the contour to light or dark voxels. Edge detection controlled by w_e and curvature used for termination controlled by w_t.

$$E_{int} = \alpha(s) \left| \frac{d\mathbf{v}(s)}{ds} \right|^2 + \beta(s) \left| \frac{d^2\mathbf{v}(s)}{ds^2} \right|^2 \quad (9)$$

$$E_{ext} = w_l \mathbf{I} + w_e |\nabla \mathbf{I}|^2 + w_t E_c(\mathbf{I}) \quad (10)$$

VI. FEATURE SELECTION

Commonly large datasets contain some features in the input space will be have no effect upon or even reduce the performance of a classifier. It is naive to use just the raw image data. Tumour features for extraction have been considered in section III which already removes some redundant information. Mapping input data into a lower dimensional space is possible and can improve performance but if ill-applied can remove key features. A brute-force approach would find the optimal combination of features but the input space is expected to be too large, 2^n, to be completely shattered within reasonable execution time.

A. Sequential Floating Search (SFS)

This heuristic algorithm is applied to tumour classification in [3]. It is possible to start from either the full or empty set of features then iteratively add and remove features to improve the performance of the classifier. A performance function is required for feature set comparison. Listing 1 contains the algorithm starting from an initial subset of no features and repeated until convergence.

```
1.    Z = {}, Y = {All}    // Setup
2.    Z = Z + Y(Best)      // Add the best feature
3.    X = Z − Z(Worst)     // Remove the worst
4.    if(f(X) > f(Z))
          Z = X
          goto 3           // Keep removing features
      else
          goto 2           // Repeat
```

Listing 1.   SFS Algorithm

B. Stochastic Approaches

A Random Mutation Hill Climber (RMHC) can move between in the combinatorial feature selection space from an initial starting point but will never reduce in performance. This does not handle a landscape with many local maxima well and may not produce a reasonable solution. Genetic algorithms are more computationally expensive as they require a population of solutions using crossover and mutation to converge on a suitable solution. Whether it out performs a RMHC depends on the landscape but using a population of solutions is certainly more thorough. Simulated annealing can be used to move between solution neighbours subject over a fixed number of iterations. A cooling schedule is used to except negative moves in performance with a probability that is a function of the cooling variable.

C. Principle Component Analysis (PCA)

PCA is a common technique used for dimensionality reduction by ranking dimensions in order of variance [23]. This will rank the features so that only the first L are passed on for further processing. The other dimensions can simply be removed but if the effect of a low variance dimension is important to classification this can reduce performance. Eq. (11) shows how the original input pattern is mapped to a reduce pattern by subtracting the mean of all patterns and

multiplying with the projection matrix. The projection matrix is built by finding the covariance matrix of the input patterns then ranking the eigenvectors by the eigenvalues and deleting as required. Performance feedback from training can be used to select appropriate L value.

$$z = P(x - \mu) \tag{11}$$

VII. CLASSIFICATION

Classification must differentiate between extracted geometric shapes that are normal and those which may potentially be tumours. Tumours will also be attached to normal internal body parts so the classifier must be able to handle any abnormalities in organs. Supervised techniques for classification are considered even though datasets have not yet been sourced.

A. Artificial Neutral Networks (ANNs)

ANNs contain summation nodes where data is propagated through weighted connections resulting in a final output. As a supervised technique weights are trained by propagating the error backwards through the network. Multilayer nets can provided non-linear separation functions and increasing the number of layers only increases possible function complexity. Neural networks have been applied successfully to classification of brain tumours [24].

Eq. (12) is an example of a two layer network with an n dimensional input space and m hidden nodes. A $tanh$ activation function is used on the output of the hidden nodes but only the sign is used for the binary classification task. There is also a scalar offset, b, on the output and an offset vector, c, on the hidden layer.

$$y = sign\left(b + \sum_{i=1}^{m} u_i \tanh\left(c_i + \sum_{j=1}^{n} x_j w_{j,i}\right)\right) \tag{12}$$

B. Support Vector Machines (SVMs)

An SVM classifier builds a separation margin supported by the closest data points then draws a separation plane from the middle of this margin. A linear maximum-margin hyperplane is produce but non-linear data can also be separated by using the kernel trick [25]. This is a mapping of the input space into a higher dimensional space so that it becomes linearly separable. SVMs have been successfully applied to breast cancer diagnosis [26]. The approach uses a weighted combination of polynomial and radial basis functions to improve the generalisation performance.

C. Boosting

A weak learner for binary classification can be considered any classifier with an error rate less than 0.5. It is possible to create a strong learner, having a much smaller error rate, by combing the weighted sum of different weak hypothesises provided by weak learners. The algorithm can be considered a hybrid of feature selection and classification.

AdaBoost is the most common implementation of a boosting algorithm and has been successfully applied to brain tumour classification [27], [28]. The architecture of AdaBoost can be thought of as single layer ANN but trained using the error in each weak hypothesis with an input dimensions equivalent to the number of boosting rounds. The weights for each hypothesis is calculated using Eq. (13) where ϵ_t is the error which means anything greater than 0.5 is negative and as $\epsilon_t \to 0$ then $\alpha_t \to \infty$. The distribution of data to train the weak learner for the next hypothesis is also determined using Eq. (13) therefore contributing to feature selection.

$$\alpha_t = \frac{1}{2} \ln\left(\frac{1 - \epsilon_t}{\epsilon_t}\right) \tag{13}$$

VIII. CONCLUSIONS

It is clear that this tool can't be used as a hard and fast method of tumour diagnosis but instead as a valuable tool for image reviewers. Software packages designed for medical image review have bidirectional interfaces to custom extensions [11]. Implementing this system as an extension would remove some overheads required for data handling but reduce the scope for optimisation. The feedback from the entire process would be a checklist which the user must manually review and waive if incorrectly identified.

Medical images are high resolution but noise can still be issue and a pre-processing stage is reasonable. The acquisition method should be verified to contain no image processing as this could produce redundancy. Anisotropic diffusion is recommended to reduce noise because edge detection is important in later stages. This method can also by easily tuned by limiting iterations of the algorithm.

Edge detection is for required for both pre-processing and feature extraction. Canny edge detection produces significantly better results than simple filter kernels but at the expense of computation. Edge, curvature and active contour feature extraction techniques are recommended for implementation. A HT would provided much noisy data which would detrimental to later stages. To deal with amount of features PCA can be used to remove redundant components but also AdaBoost in conjunctions with the classifier algorithm. SVMs are robust machine learning architectures and should defiantly provide at least weak hypothesises capable which should prove useful in the boosting algorithm.

The confidence analysis unit will take noise information from the initial image by differencing the input and output of the pre-processing stage. In feature extraction it can report on the quantity of extraction from an image. Dimensionality reduction will have no output as the reduction value is tuned prior to deployment. The binary classifier also a non-discreet output which can used be used as a measure of confidence. This can also be used to adaptively control the number of boosting rounds.

REFERENCES

[1] S. Ahmed, K. Iftekharuddin, and A. Vossough, "Efficacy of texture, shape, and intensity feature fusion for posterior-fossa tumor segmentation in mri," *Info Tech in BioMed, IEEE Trans on*, vol. 15, no. 2, pp. 206–213, March 2011.

[2] V. Kumar, J. Sachdeva, I. Gupta, N. Khandelwal, and C. Ahuja, "Classification of brain tumors using pca-ann," in *Info and Comms Tech (WICT), 2011 World Congress on*, Dec 2011, pp. 1079–1083.

[3] H.-L. Bu, G.-Z. Li, X.-Q. Zeng, J. Yang, and M. Yang, "Feature selection and partial least squares based dimension reduction for tumor classification," in *Bioinformatics and Bioengineering, 2007. BIBE 2007. Proceedings of the 7th IEEE International Conference on*, Oct 2007, pp. 967–973.

[4] J. Sachdeva, V. Kumar, I. Gupta, N. Khandelwal, and C. Ahuja, "Multiclass brain tumor classification using ga-svm," in *Developments in E-systems Eng. (DeSE), 2011*, Dec 2011, pp. 182–187.

[5] W. Kostis, A. Reeves, D. Yankelevitz, and C. Henschke, "Three-dimensional segmentation and growth-rate estimation of small pulmonary nodules in helical ct images," *Med Imaging, IEEE Trans on*, vol. 22, no. 10, pp. 1259–1274, Oct 2003.

[6] K. Najarian and R. Slinter, *Biomedical Signal and Image Processing*, 1st ed. Taylor and Francis Group, 2006.

[7] H. L. Liu, O. Elhage, P. Dasgupta, B. Challacombe, D. Murphy, L. Seneviratne, and K. Althoefer, "A haptic probe for soft tissue abnormality identification during minimally invasive surgery," in *Reconfigurable Mechanisms and Robots, 2009. ReMAR 2009. ASME/IFToMM International Con. on*, June 2009, pp. 417–422.

[8] P. S. Wellman and R. D. Howe, "Modeling probe and tissue interaction for tumor feature extraction," *ASME-PUBLICATIONS-BED*, vol. 35, pp. 237–238, 1997.

[9] NEMA. (2011) DICOM. [Visited] 13/03/14.

[10] FNLCR. The cancer imaging archive. [Visited] 16/03/14. [Online]. Available: http://cancerimagingarchive.net/

[11] 3DSlicer. [Visited] 13/03/14. [Online]. Available: http://www.slicer.org/

[12] G. Cooper, *Elements of Human Cancer*, ser. Biology Series. Jones and Bartlett Publishers, 1992.

[13] R. Islam, A. Mamun, M. Bhuiyan, and S. Rahman, "Segmentation and 3d visualization of volumetric image for detection of tumor in cancerous brain," in *Elec Comp Eng (ICECE), 2012 7th Int. Con.*, Dec 2012, pp. 863–866.

[14] A. Amutha and R. Wahidabanu, "Lung tumor detection and diagnosis in ct scan images," in *Comms and Sig. Proc. (ICCSP), 2013 Int. Con.*, April 2013, pp. 1108–1112.

[15] Y. Chen, R. Xu, S.-Y. Tang, S. Morikawa, and Y. Kurumi, "Non-rigid mr-ct image registration for mr-guided liver cancer surgery," in *Complex Med Eng, 2007. CME 2007. IEEE/ICME Int. Con. on*, May 2007, pp. 1756–1760.

[16] G. Lohmann, *Volumetric Image Analysis*, 1st ed. Wiley, 1998.

[17] G. Harauz and M. van Heel, "Exact filters for general geometry three dimensional reconstruction," in *Proceedings of the IEEE Computer Vision and Pattern Recognition Conf*, vol. 73, 1986, pp. 146–156.

[18] M. Nixon and A. Aguado, *Feature Extraction and Image Processing*, 1st ed. Newnes, 2002.

[19] B. Nakhjavanlo, T. Ellis, P. H. Soan, and J. Dehmeshki, "3d medical image segmentation using level set models and anisotropic diffusion," in *Signal-Image Technology and Internet-Based Systems (SITIS), 2011 Seventh International Conference on*, Nov 2011, pp. 403–408.

[20] J. Canny, "A computational approach to edge detection," *Pattern Analysis and Machine Intelligence, IEEE Transactions on*, vol. PAMI-8, no. 6, pp. 679–698, Nov 1986.

[21] A. Abuzaina, T. Alathari, M. Nixon, and J. Carter, "Detecting moving spheres in 3d point clouds via the 3d velocity hough transform," in *IVMSP Workshop, 2013 IEEE 11th*, June 2013, pp. 1–4.

[22] A. Skalski, J. Lagwa, P. Kedzierawski, T. Zielinski, and T. Kuszewski, "Automatic prostate segmentation in mr images based on 3d active contours with shape constraints," in *Signal Processing: Algorithms, Architectures, Arrangements, and Applications (SPA), 2013*, Sept 2013, pp. 246–249.

[23] K. Pearson, "On lines and planes of closest fit to systems of points in space," *Phil. Mag.*, vol. 6, pp. 559–572, 1901.

[24] S. E. Amin and M. A. Megeed, "Brain tumor diagnosis systems based on artificial neural networks and segmentation using mri," in *Informatics and Systems (INFOS), 2012 8th International Conference on*, May 2012, pp. MM–119–MM–124.

[25] C. Cortes and V. Vapnik, "Support-vector networks," *Machine learning*, vol. 20, no. 3, pp. 273–297, 1995.

[26] X. Yang, H. Peng, and M. Shi, "Svm with multiple kernels based on manifold learning for breast cancer diagnosis," in *Information and Automation (ICIA), 2013 IEEE International Conference on*, Aug 2013, pp. 396–399.

[27] Y. Freund and R. E. Schapire, "A short introduction to boosting," vol. 14, no. 5, Sep 1999, pp. 771–780.

[28] A. Islam, S. Reza, and K. Iftekharuddin, "Multifractal texture estimation for detection and segmentation of brain tumors," *Biomedical Engineering, IEEE Transactions on*, vol. 60, no. 11, pp. 3204–3215, Nov 2013.